

2D Basement Relief Inversion using Sparse Regularization.

Francisco Márcio Barboza
Department of Computing and Technology
Federal University of Rio Grande do Norte
Caicó, Rio Grande do Norte
marcio.barboza@ufrn.br

Arthur Anthony da Cunha Romão E Silva
Graduate Program on Systems and Computing
Federal University of Rio Grande do Norte
Natal, Rio Grande do Norte
arthur.romao@ufrn.br

Bruno Motta de Carvalho
Department of Informatics and Applied Mathematics
Federal University of Rio Grande do Norte
Natal, Rio Grande do Norte
bruno@dimap.ufrn.br

Abstract—Basement relief gravimetry is a key application in geophysics, particularly important for oil exploration and mineral prospecting. It involves solving an inverse geophysical problem, where the parameters of a geological model are inferred from observed data. In this context, the geological model consists of the depths of constant-density prisms representing the basement relief, and the data correspond to the gravitational anomalies caused by these prisms. Inverse geophysical problems are typically ill-posed, as defined by Hadamard, meaning that small perturbations in the data can result in large variations in the solutions. To address this instability, regularization techniques, such as those proposed by Tikhonov, are employed to stabilize the solutions. This study presents a comparative analysis of various regularization techniques applied to the gravimetric inversion problem, including Smoothness Constraints, Total Variation, the Discrete Cosine Transform (DCT), and the Discrete Wavelet Transform (DWT) using Daubechies D4 wavelets. Optimization methods are commonly used in inverse geophysical problems because of their ability to find optimal parameters that minimize the objective function—in this case, the depths of the prisms that best explain the observed gravitational anomalies. The Genetic Algorithm (GA) was selected as the optimization technique. GA is based on Darwinian evolutionary theory, specifically the principle of natural selection, where the fittest individuals in a population are selected to pass on their traits. In optimization, this translates to selecting solutions that most effectively minimize the objective function. The results, evaluated using fit metrics and cumulative error analysis, demonstrate the effectiveness of all the regularization techniques used and the Genetic Algorithm. Among the methods tested, the Smoothness constraint was briefly the most effective for the first and second synthetic models. For the third model, which was based on real data, all regularization methods performed equivalently.

Keywords—gravimetric inversion; genetic algorithm; regularization.

I. INTRODUCTION

The identification of geological features in basement topography is of great importance to the oil industry [1]. The study of basement topography in sedimentary basins aids in the

search for oil and gas accumulations. A gently undulating basement topography, or one locally marked by a series of small-offset faults, can lead to the trapping of a reservoir rock layer between impermeable rock layers and the basement, forming a stratigraphic trap for oil [2]. Therefore, studying basement topography is crucial for identifying potential oil traps.

Estimating the topography is an inverse problem, as it involves estimating the heights of basement topography prisms from observed gravity data. According to [3], an inverse problem is considered ill-posed if it is characterized by the absence, non-uniqueness, or instability of solutions. The gravimetric inverse problem of estimating basement topography is ill-posed because its solution is not unique and is unstable. To transform it into a well-posed problem, the incorporation of *a priori* geological information is required. This is commonly achieved by adding a regularizing term to the functional [4].

Gravimetric data interpretation can utilize inversion methods. For example, the inversion method using the smoothness regularizer (SV) [4] can be applied to estimate the topography of sedimentary basins with smooth basements. However, to estimate abrupt discontinuities in the basement topography of sedimentary basins, it is recommended to apply inversion methods that incorporate total variation (TV) constraints, such as those proposed by [5] and [6].

This work addresses the estimation of both smooth and non-smooth solutions for the gravimetric inverse problem of estimating the topography of a sedimentary basin. Regularization methods commonly used in geophysical inversion aim to reconstruct smooth solutions, even though geological structures often exhibit sharp contrasts (discontinuities) in physical properties.

The article by [7] addresses the regularization of geophysical ill-posed problems, both linear and non-linear, using joint

sparsity constraints. We introduce the sparsity constraint using the discrete cosine transform (DCT) and discrete wavelet transforms (DWT) of the Daubechies D4 type [8] for this inverse problem. These constraints allow the reconstruction of sparse solutions in the DCT and wavelet domains. This approach enables the reconstruction of non-smooth density functions that represent abrupt geological structures. The sparsity constraint is particularly important because it allows for solutions that exhibit sharp edge definitions of anomalous bodies [9].

An inversion algorithm based on the genetic algorithm was implemented in MATLAB to solve the inverse problem using various constraints.

We applied the proposed methodology, using smoothness, total variation, and sparsity constraints, to synthetic data produced by two simulated geological environments with abrupt discontinuities in basement topography. Additionally, we applied the proposed method to real data from the Ponte do Poema, located at the UFPA Belém Campus. The synthetic and real models were based on the works of [10] and [2], respectively. The objective was to identify which constraint best regularized the problem and provided the best fit to the observed data.

II. METHODOLOGY

It is assumed that a sedimentary basin consists of homogeneous basement rocks and heterogeneous sediments. Let g be a set of N gravimetric observations inserted into a Cartesian plane. We assume that the density contrast $\Delta\rho$ between the sediment and the basement is constant and known. From these observations, comparisons between the density of the basement topography S and the sedimentary material are generated.

The z axis is positive vertically downward in the Cartesian coordinate system. The sediment of a basin is approximated by a rectangular matrix of M vertically juxtaposed 2D rectangular prisms, whose tops coincide with the ground surface. The horizontal dimensions of all prisms are constant and known. The depths of the bases of the prisms p_j (with $j = 1, \dots, M$) represent the depths of the basement.

The gravity anomaly g_i at the i -th observation point caused by a set of prisms is given by the non-linear relationship:

$$g_i = \sum_{j=1}^M f_i(\Delta\rho_j, p_j, r_{ij}), \quad i = 1, 2, \dots, N \quad (1)$$

The non-linear function $f_i(\Delta\rho_j, p_j, r_{ij})$ calculates the gravitational anomaly caused by the j -th prism at the i -th observation point. That is, it solves the forward problem for an individual prism at observation point i . Here, $\Delta\rho_j$ is the density contrast of the j -th prism, p_j is the depth of the j -th prism, and r_{ij} is the horizontal position vector between the i -th point and the j -th prism [11].

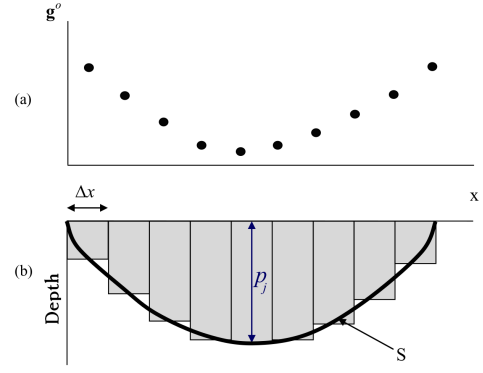


Figure 1. (a) Gravimetric anomaly and (b) sedimentary basin showing basement topography S and an interpretive model formed by a set of M juxtaposed 2D rectangular prisms with height p_j .
Source: [2]

The objective is to estimate S considering, as an interpretive model, a set of M vertical rectangles juxtaposed along the x -axis of the Cartesian plane. The depths p_j of the rectangles are the parameters to be estimated. The apex of each rectangle is located at the Earth's surface, collectively forming a flat ground, and all rectangles have the same horizontal distances Δx [10].

A. Inverse Problem

According to [12], the geophysical problem of gravimetric inversion can be formulated as the minimization of the functional ϕ , described by the equation:

$$\phi(p) = \frac{\|g^{obs} - g(p)\|_2^2}{N f_\phi}, \quad (2)$$

where p is the depth vector defined as $p = (p_1, p_2, \dots, p_M)$, $g^{obs} = (g_1^{obs}, g_2^{obs}, \dots, g_N^{obs})$ represents the set of observed gravity measurements, and $g(p) = (g_1, g_2, \dots, g_N)$ is the set of calculated gravity values based on Equation 1. Here, N denotes the number of observations [13, 12], and f_ϕ is a normalization factor. It is assumed that ϕ is non-linear, continuous, and has continuous first and second derivatives with respect to p .

B. Regularization

The problem of minimizing $\phi(p)$ is ill-posed when finding the vector p and minimizing $\phi(p)$, as the obtained solutions generally exhibit instability. To regularize the problem, a constraint is used, which is *a priori* information added with the aim of regularizing the problem [12].

Regularization can be understood as the approximation of an ill-posed problem to a family of quasi-solutions [4]. The objective of regularization is to try to circumvent the violation of one or more Hadamard conditions [14]. The objective function added with a constraint then becomes:

$$\Omega(p) = \phi(p) + \alpha \frac{\mathcal{R}(p)}{f_{\mathcal{R}}}, \quad (3)$$

where ϕ is the functional described in Equation 2, α is the Lagrange multiplier, \mathcal{R} is the constraint that aims to regularize the solution, and $f_{\mathcal{R}}$ is the normalization factor of the constraint.

1) *Smoothness*: One of the regularizations used in this work is the one adopted by [4]. The objective of the smoothness constraint is to stabilize a solution by favoring a smooth behavior [10, 11, 15].

Therefore, the inversion process uses a Lagrange multiplier multiplied by the constraint, and this product is added to ϕ from Equation 2. Thus, the inverse geophysical problem is described as:

$$\Omega(p) = \phi(p) + \alpha \frac{\mathcal{R}_{suav}(p)}{f_{\mathcal{R}_{suav}}}, \quad (4)$$

where

$$\mathcal{R}_{suav}(p) = \|\mathcal{S}p\|_2^2, \quad (5)$$

and where α is the Lagrange multiplier, \mathcal{R}_{suav} is the smoothness constraint, \mathcal{S} is the finite difference matrix, and p is the vector of depths of the prisms representing the basin.

2) *Total Variation*: For the proposed problem, minimizing the squared L_2 norm of the depth vector multiplied by the finite difference matrix provides estimates of smooth and undulating topography, whereas minimizing the L_1 norm of the same product results in estimates that favor discontinuities [10, 2, 15].

The total variation (TV) constraint uses the L_1 norm, and the inverse geophysical problem can be described as:

$$\Theta(p) = \phi(p) + \alpha \frac{\mathcal{R}_{TV}(p)}{f_{\mathcal{R}_{TV}}}, \quad (6)$$

where

$$\mathcal{R}_{TV}(p) = \|\mathcal{S}p\|_1, \quad (7)$$

where α is the Lagrange multiplier, \mathcal{R}_{TV} is the TV constraint, \mathcal{S} is the finite difference matrix, and p is the vector of depths of the prisms.

3) *Sparsity*: The sparsity constraint uses the Discrete Cosine Transform (DCT) and the Discrete Wavelet Transform (DWT), and employs the L_1 norm to achieve a sparse model [7, 16, 15].

A wavelet can be described as a small wave, complementing the classical Fourier decomposition method (which uses large sinusoidal waves), and in essence, it is an oscillation that decays rapidly [17]. The use of DCT results in decorrelation of data, removing redundancy among neighboring data points [18].

Both DCT and DWT constraints use the L_1 norm, resulting in a sparse model in inversion. The inverse geophysical problem with sparsity constraint is defined as:

$$\Psi(p) = \phi(p) + \alpha \frac{\mathcal{R}_{esp}(p)}{f_{\mathcal{R}_{esp}}}, \quad (8)$$

where

$$\mathcal{R}_{esp}(p) = \|\mathcal{E}p\|_1, \quad (9)$$

where α is the Lagrange multiplier, \mathcal{R}_{esp} is the sparsity constraint, p is the vector of depths of the basin, and \mathcal{E} is the matrix of the transform, such as the Discrete Wavelet Transform (DWT) or the Discrete Cosine Transform (DCT).

C. Genetic Algorithms

Genetic Algorithms are search algorithms based on mechanisms of natural selection and genetics [19]. The purpose of the algorithm is to indicate a potential solution to a specific problem using a data structure similar to chromosomes and applying recombination of these structures to preserve critical information. Additionally, genetic algorithms are often seen as metaheuristic global optimization techniques.

The goal of the algorithm is to iteratively generate increasingly evolved populations through evolutionary rules or genetic operations in pursuit of an optimal result. A population becomes more evolved when its individuals are better adapted to the environmental conditions. In solving the inverse problem, for instance, the smaller the value of the function for individuals in the population, the better adapted they are, implying a more evolved population. The initial population is generated randomly or based on information from the problem to be optimized [20].

Initially, an initial population is generated with a set of random chromosomes. Each chromosome represents a possible solution, which is then evaluated to assign a score based on desired characteristics. The best solutions are selected (elitism), and new chromosomes are generated through crossover between chromosomes from the previous iteration and/or mutations. This process is repeated until the algorithm's stopping criterion is met. If we define $pop(t)$ as a population of chromosomes at generation t , the standard pseudocode of the genetic algorithm is outlined in Algorithm 1 as described by [19].

In this study, the population size was 1,000, the maximum number of iterations was 1,000, the tournament size was 3, the mutation rate was 1%, and the mutation magnitude was 10%. The crossover rate was 75%, the lower bound was a vector of zeros with the size corresponding to the number of parameters to be estimated, and the upper bound was a vector with the same number of parameters, but with a fixed value of 4, based on a maximum depth estimate of the synthetic and real models studied. These parameters encompass a more

Algoritmo 1: Standard Genetic Algorithm

Initialize $pop(t)$
Evaluate $pop(t)$
while stopping criterion not satisfied **do**
 $t \leftarrow t + 1$
 Select $pop(t)$ from $pop(t - 1)$
 Apply crossover in $pop(t)$
 Apply mutation in $pop(t)$
 Apply elitism in $pop(t)$ from $pop(t - 1)$
 Evaluate $pop(t)$
end while

comprehensive version of the Genetic Algorithm, as detailed by the authors [19, 21, 22, 23, 24].

III. RESULTS AND DISCUSSION

In this section, two synthetic models simulating gravimetric anomalies in sedimentary basins are presented. Both models are two-dimensional, with constant density contrast, geologically smooth, but featuring significant discontinuities that are to be estimated through inversion.

Gravimetric data from these synthetic models were generated and had 5% pseudo-random Gaussian noise added to simulate the variations typically observed during field measurements.

Additionally, real data collected from the Ponte do Poema, located at the Federal University of Pará, Belém Campus, were used to validate the inversion methods applied in this study. The Ponte do Poema was chosen for its strategic location and structural characteristics, which provide stable conditions for gravimetric measurements. This real data offers a practical context for evaluating the performance of the proposed inversion techniques, providing insight into how these methods function under real-world conditions.

For each model, 10 inversions were conducted for each of the four constraints addressed in this study. From the inversion results, the average solution for each constraint was calculated, resulting in different mean models with distinct characteristics depending on the applied constraint. The Lagrange multipliers (α) for each constraint were determined using the L-curve method [25].

Moreover, figures showing the convergence of functionals from the inversions with each proposed constraint are presented. It is important to note that each figure represents an example of a single inversion for each constraint, aiming to illustrate the behavior of the functionals. However, the isolated functionals do not represent the optimal solution, as they do not fully integrate the constraints. Nonetheless, they exhibit values that are close to one another, considering the scale of the graphs.

A. Isolated Graben

For this model, a constant density contrast of -0.25 g/cm^3 was established. The horizontal extent of the model is 60 km, using 60 prisms, and the maximum depth reaches 1.85 km.

Figure 2 synthetically presents a model of a sedimentary basin with an isolated graben at the center of the measurements, as described by [10]. Gravimetric measurements were generated based on this synthetic model.

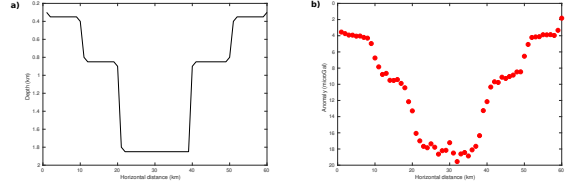


Figure 2. (a) True synthetic model of isolated graben and (b) observed gravimetric data set from the model in question.

The Figure 3 presents the result of the average of 10 inversions estimated based on observed gravimetric data, along with the true synthetic model for comparison in each constraint. The Lagrange multipliers were $\alpha = 8 \times 10^{-1}$ for DCT, $\alpha = 8 \times 10^{-1}$ for TV, $\alpha = 9 \times 10^{-1}$ for DWT, and $\alpha = 2 \times 10^0$ for SV. The normalization factors are shown in Table III-A.

Ω	Θ	Ψ_{DCT}	Ψ_{DWT}
$f_{\phi} = 1.5$	$f_{\phi} = 1.5$	$f_{\phi} = 1$	$f_{\phi} = 0.95$
$f_{R_{suav}} = 1$	$f_{R_{TV}} = 1$	$f_{R_{DCT}} = 1.1$	$f_{R_{DWT}} = 1.2$

Table I

NORMALIZATION FACTORS FOR THE ISOLATED GRABEN MODEL.

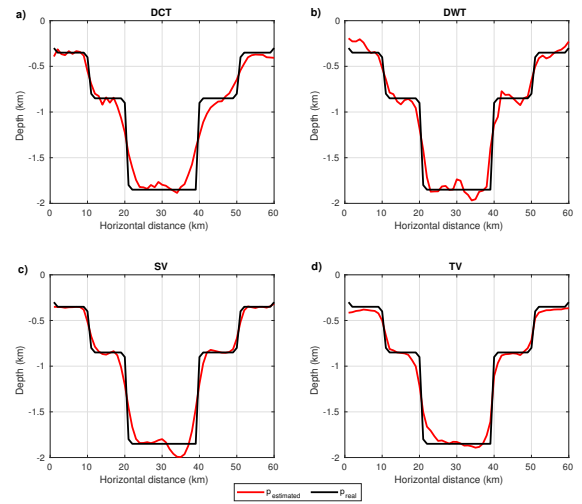


Figure 3. Result of the average of 10 inversions of the isolated graben model using constraint (a) DCT, (b) DWT, (c) SV, and (d) VT.

The estimated parameters, as shown in Figure 3, indicate a good fit among the constraints. For a more detailed analysis,

the relative error between the data estimated by the average of inversions and the data from the true synthetic model was calculated, as shown in Figure 4.

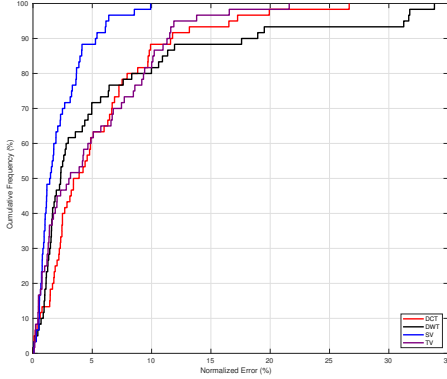


Figure 4. Relative error between the data from the true isolated graben model and the average of 10 inversions in each addressed constraint.

Figure 4 shows that the best results, based on the average of inversions, were achieved with the DCT constraint, where 89% of the data contributed to approximately 10% of the error. The TV constraint produced an average inversion error of about 12%, also associated with 89% of the data. For the DWT constraint, the average error was around 13%, with 89% of the data considered. The best overall result came from the SV constraint, where 89% of the data accounted for only about 4% of the error.

Figure 5 illustrates the inversion functional, which graphically represents the difference between observed data and estimated data, considering the constraint used.

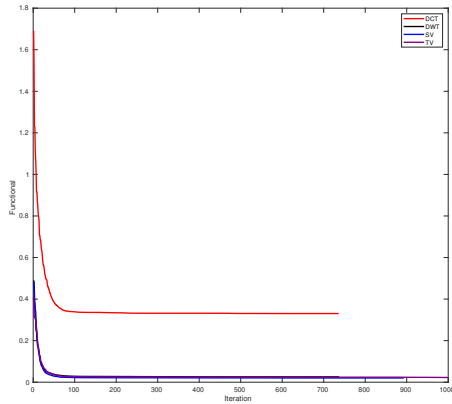


Figure 5. Convergence curve of the functional with the constraints used in the inversion of gravimetric data from the isolated graben model.

Figure 5 shows the convergence of the functional discussed in Equation 3. It can be observed that there was good and equivalent convergence of functionals among the constraints.

B. Two Sub-basins

For this model, a constant density contrast of -0.25 g/cm^3 was established. The horizontal extent of the model is 80 km, using 80 prisms, and the maximum depth reaches 3.5 km.

Figure 6 synthetically presents a model of a sedimentary basin with two consecutive and closely spaced sub-basins, as described by [10]. Gravimetric measurements were generated based on this synthetic model.

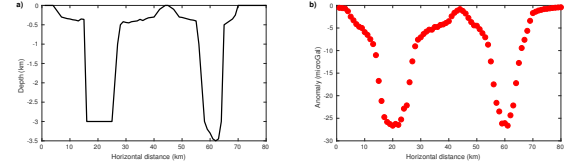


Figure 6. (a) True synthetic model of two sub-basins and (b) observed gravimetric data set from the model in question. In (b), it is noticeable that the depocenter of the left basin has greater curvature than the depocenter of the right basin.

Figure 7 presents the result of averaging 10 inversions estimated based on the observed gravimetric data, along with the true synthetic model for comparison under each constraint. The Lagrange multipliers were $\alpha = 1 \times 10^{-1}$ for DCT, $\alpha = 1 \times 10^{-1}$ for TV, $\alpha = 3 \times 10^{-2}$ for DWT, and $\alpha = 25 \times 10^{-2}$ for SV. The normalization factors are shown in Table III-B.

Ω	Θ	Ψ_{DCT}	Ψ_{DWT}
$f_\phi = 1.6$	$f_\phi = 1.6$	$f_\phi = 2.1$	$f_\phi = 1.26$
$f_{\mathcal{R}_{suav}} = 1$	$f_{\mathcal{R}_{TV}} = 1$	$f_{\mathcal{R}_{DCT}} = 1.25$	$f_{\mathcal{R}_{DWT}} = 1.15$

Table II

NORMALIZATION FACTORS FOR THE TWO SUB-BASINS MODEL.

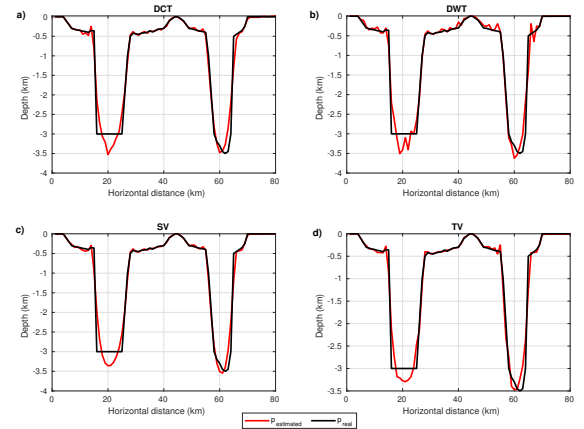


Figure 7. Result of averaging 10 inversions of the two sub-basin model using (a) DCT, (b) DWT, (c) SV, and (d) TV constraints.

It is observable from Figure 7 that the constraints were successful in regularization. For a more detailed analysis of the results, Figure 8 shows the relative error between the estimated

data from each inversion and the data from the true synthetic model.

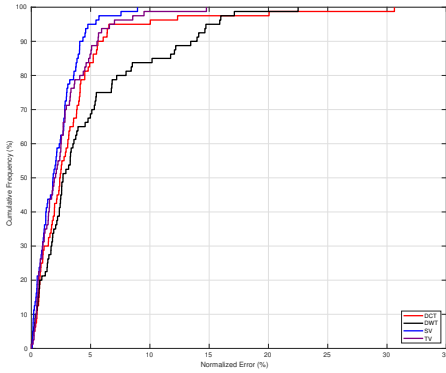


Figure 8. Relative error between true two sub-basin model data and the average of 10 inversions under each constraint.

Figure 8 shows that the best result from the average of inversions was achieved with the SV constraint, where 94% of the data accounted for approximately 4% of the error. Inversions using the TV and DCT constraints resulted in around 5.3% error, also associated with 94% of the data. Finally, the DWT constraint produced approximately 17% error, associated with 90% of the data.

Figure 9 illustrates the functional of the inversions, graphically representing the difference between observed and estimated data, considering the constraint used.

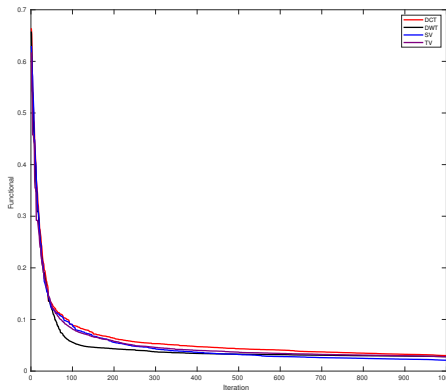


Figure 9. Convergence curve of the functional with the constraints used in the inversion of gravimetric data for the two sub-basin model.

Figure 9 shows the convergence of the functional discussed in Equation 3. It is evident that there was good and equivalent convergence of the functionals.

C. Bridge of the Poema

According to the works of [10] and [2], the methodologies of gravimetric inversion were applied in this study to the observed

data at Bridge of the Poema, located at the Belém Campus of the Federal University of Pará.

Figure 10 shows a photograph of the relief of Bridge of the Poema, with the topographic gradients g_1 and g_2 , and the reinforcement piles A and B, which are also considered sources of the gravimetric anomaly [10].

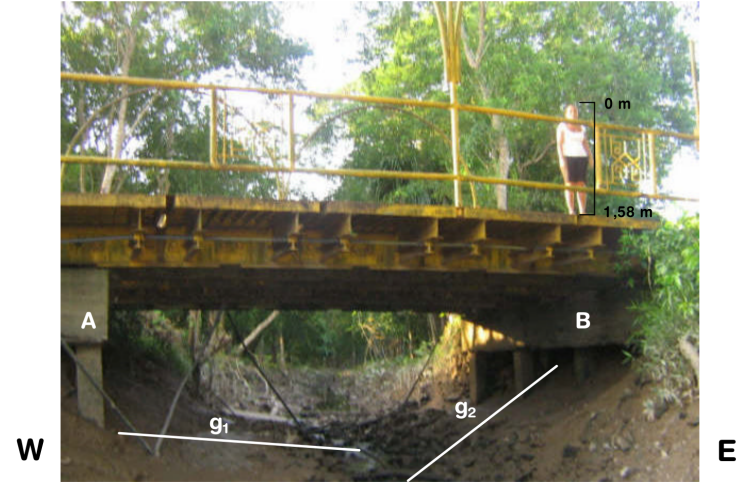


Figure 10. Photograph with W-E gravimetric profile of Bridge of the Poema. The west side has a sharper discontinuity compared to the east side. Source: [26].

For this interpretative model, a constant density contrast of -2.3 g/cm^3 was adopted. The horizontal extent of the model is 21.5 m, using 45 prisms. The maximum depth of the relief, estimated from the photograph in Figure 10, is 3.3 m, as described by [26].

Figure 11 presents the result of averaging 10 inversions estimated based on gravimetric data using all constraints. The Lagrange multiplier had a value of $\alpha = 2 \times 10^{-3}$ for TV, $\alpha = 1 \times 10^{-3}$ for SV, $\alpha = 6 \times 10^{-3}$ for DCT and DWT. The normalization factors are shown in Table III-C.

Ω	Θ	Ψ_{DCT}	Ψ_{DWT}
$f_\phi = 1$	$f_\phi = 1.5$	$f_\phi = 1$	$f_\phi = 1$
$f_{R_{sav}} = 1$	$f_{R_{TV}} = 1$	$f_{R_{DCT}} = 1$	$f_{R_{DWT}} = 1$

Table III
NORMALIZATION FACTORS FOR THE POEMA BRIDGE MODEL.

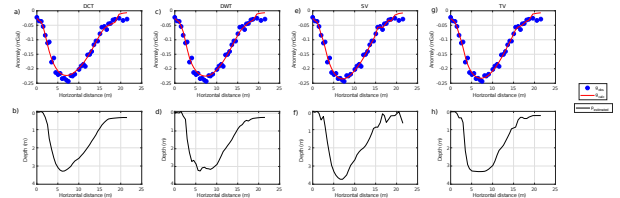


Figure 11. Result of averaging 10 inversions with constraints. Set of gravimetric observations (blue dots) and calculated (red line) from DCT, DWT, SV, and TV constraints, as in (a), (c), (e), and (g), respectively. Inversely estimated model by DCT, DWT, SV, and TV constraints, as in (b), (d), (f), and (h), respectively.

It is notable that all constraints were effective in regularization, and there was a good fit between observed and calculated data, resulting in a model estimate that is quite similar across the adopted constraints. For further evaluation of the best results, refer to Figure 12, which shows the relative error between the average calculated gravities from each inversion and the observed gravimetric data:

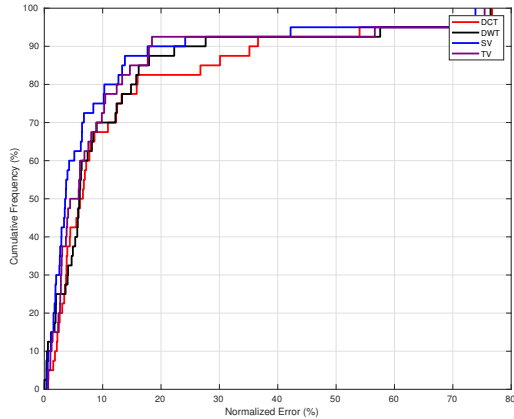


Figure 12. Relative error between the gravimetric data of the Bridge of the Poema model and the average calculated gravities from 10 inversions with each addressed constraint.

In Figure 12, it can be observed that for inversions using TV and SV constraints, approximately 90% of the data accounted for around 17% error in relation to the observed gravities. For DWT and DCT, 80% of the data accounted for 14% error.

Figure 13 displays the functionals of the inversions, showing excellent and equivalent convergence among the functionals with the addressed constraints.

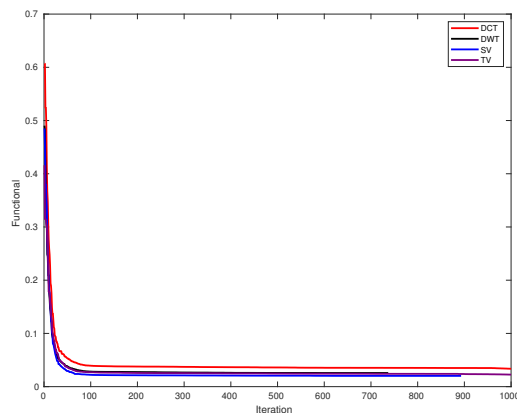


Figure 13. Convergence curve of the functional with the constraints used in the inversion of gravimetric data from the Bridge of the Poema model.

The limited number of parameters (approximately 100) may

have constrained the efficiency of the sparsity enforcement, as models with fewer parameters tend to be less sparse in the DCT or DWT domain.

IV. CONCLUSION

This study demonstrates the effectiveness of various regularization methods and optimization techniques in addressing the gravimetric inversion problem for 2D basement relief. Among the analyzed methods, the Smoothness regularization technique proved to be the most effective in two synthetic models, briefly reducing the error between the observed and calculated data. However, in the Poema Bridge model, all constraints performed equally well, with a slight advantage over the sparse constraints. Although the Discrete Cosine Transform (DCT) and Discrete Wavelet Transform (DWT) with Daubechies D4 wavelets were less effective in this particular case, their sparse regularization capabilities may perform better in problems involving a larger number of parameters. In this study, the relatively small number of parameters (around 100) may have limited the effectiveness of these techniques. The Genetic Algorithm used for optimization also performed well, efficiently minimizing the objective function and confirming its suitability for solving inverse geophysical problems. Future research could explore the performance of DCT and DWT in more complex models with higher parameter counts, where their ability to impose sparsity may lead to improved outcomes. In gravity inversion, the incorporation of regularization constraints is crucial to obtain interpretable models, as their absence can lead to instability. In this study, all constraints were found to be optimal and equivalent, each offering distinct characteristics. For future work, it is recommended to explore multi-objective algorithms and inversion techniques in 3D models. This could significantly advance research into the application of sparsity constraints in gravity inverse problems and further validate the effectiveness of commonly used regularizers.

ACKNOWLEDGEMENTS

This study was financed in part by the Coordenação de Aperfeiçoamento de Pessoal de Nível Superior - Brasil (CAPES) - Finance Code 001.

REFERENCES

- [1] W. M. Telford, L. P. Geldart, and R. E. Sheriff, *Applied Geophysics*. Cambridge: Cambridge University Press, 1990.
- [2] R. D. C. S. d. Santos *et al.*, "Inversão gravimétrica rápida do relevo do embasamento aplicando o funcional da variação total," *Boletim de Geociências da Petrobras*, vol. 21, no. 1, pp. 45–57, 2013.
- [3] J. Hadamard, "Sur les problèmes aux dérivées partielles et leur signification physique," *Princeton university bulletin*, pp. 49–52, 1902.
- [4] A. N. Tikhonov and V. Y. Arsenin, "Solutions of ill-posed problems," *New York*, vol. 1, p. 30, 1977.

- [5] C. M. Martins, W. A. Lima, V. C. Barbosa, and J. B. Silva, "Total variation regularization for depth-to-basement estimate: Part 1—mathematical details and applications," *Geophysics*, vol. 76, no. 1, pp. I1–I12, 2011.
- [6] W. A. Lima, C. M. Martins, J. B. Silva, and V. C. Barbosa, "Total variation regularization for depth-to-basement estimate: Part 2—physicogeologic meaning and comparisons with previous inversion methods," *Geophysics*, vol. 76, no. 1, pp. I13–I20, 2011.
- [7] A. Gholami and H. Siahkoochi, "Regularization of linear and non-linear geophysical ill-posed problems with joint sparsity constraints," *Geophysical Journal International*, vol. 180, no. 2, pp. 871–882, 2010.
- [8] I. Daubechies, *Ten Lectures on Wavelets*. Philadelphia: SIAM, 1992.
- [9] C. Youzwishen and M. Sacchi, "Edge preserving imaging," *Journal of Seismic Exploration*, vol. 15, no. 1, p. 45, 2006.
- [10] W. A. Lima, "Inversão gravimétrica do relevo de bacias extencionais através da variação total," Ph.D. dissertation, Dissertação de Mestrado—Programa de Pós-Graduação em Geofísica, Instituto de Geociências, 2009.
- [11] J. B. Silva, A. S. Oliveira, and V. C. Barbosa, "Gravity inversion of 2D basement relief using entropic regularization," *Geophysics*, vol. 75, no. 3, pp. I29–I35, 2010.
- [12] J. B. Silva, W. E. Medeiros, and V. C. Barbosa, "Pitfalls in nonlinear inversion," *Pure and Applied Geophysics*, vol. 158, no. 5-6, pp. 945–964, 2001.
- [13] V. C. F. Barbosa, "Mapeamento do relevo do embasamento de bacias sedimentares através da inversão gravimétrica vinculada," Ph.D. dissertation, Universidade Federal do Pará, 1998.
- [14] H. W. Engl, M. Hanke, and A. Neubauer, *Regularization of inverse problems*. Springer Science & Business Media, 1996, vol. 375.
- [15] F. M. Barboza, W. E. Medeiros, and J. M. Santana, "A user-driven feedback approach for 2D direct current resistivity inversion based on particle swarm optimization," *Geophysics*, vol. 84, no. 2, pp. E105–E124, 2019.
- [16] R. R. d. S. Dantas, "Resolução em tomografia de tempo de trânsito poço-a-poço: a dependência da iluminação," Master's thesis, Universidade Federal do Rio Grande do Norte, 2015.
- [17] M. Sifuzzaman, M. R. Islam, and M. Ali, "Application of wavelet transform and its advantages compared to Fourier transform," *Journal of Physical Sciences*, vol. 13, no. 1, pp. 121–134, 2009.
- [18] S. A. Khayam, "The discrete cosine transform (DCT): theory and application," *Michigan State University*, vol. 114, pp. 4–8, 2003.
- [19] J. H. Holland, "Adaptation in natural and artificial systems, university of michigan press," *Ann arbor, MI*, vol. 1, no. 97, p. 5, 1975.
- [20] D. E. Golberg, "Genetic algorithms in search, optimization, and machine learning," *Addison-Wesley*, 1989.
- [21] D. E. Goldberg, J. Richardson *et al.*, "Genetic algorithms with sharing for multimodal function optimization," in *Genetic algorithms and their applications: Proceedings of the Second International Conference on Genetic Algorithms*. Hillsdale, NJ: Lawrence Erlbaum, 1987, pp. 41–49.
- [22] R. L. Haupt and S. E. Haupt, *Practical genetic algorithms with CD-Rom*. Wiley-Interscience, 2004.
- [23] K. Man, K. Tang, and S. Kwong, "Genetic algorithms: Concepts and designs, springer," 1999.
- [24] Z. Michalewicz and Z. Michalewicz, "Evolution strategies and other methods," *Genetic algorithms+ data structures= evolution programs*, pp. 167–184, 1994.
- [25] P. C. Hansen, "The L-curve and its use in the numerical treatment of inverse problems," *Computational Inverse Problems in Electrocardiology*, vol. 5, pp. 119–142, 1999.
- [26] A. d. S. Oliveira, "Inversão gravimétrica do relevo do embasamento usando regularização entrópica," *Revista Brasileira de Geofísica*, vol. 25, no. 2, pp. 207–220, 2007.